

*Department of Biology and Chemistry*  
*Faculty Publications and Presentations*

---

Liberty University

Year 2006

---

Peri-nuclear clustering of mitochondria is  
triggered during aluminum maltolate  
induced apoptosis

David A. Dewitt\*      Jennifer A. Hurd<sup>†</sup>      Nena Fox<sup>‡</sup>  
Brigitte E. Townsend\*\*      Kathleen J. S. Griffioen<sup>††</sup>  
Othman Ghribi<sup>‡‡</sup>      John Savory<sup>§</sup>

\*Liberty University, dadewitt@liberty.edu

†

‡

\*\*

††

‡‡

§

This paper is posted at DigitalCommons@Liberty University.

[http://digitalcommons.liberty.edu/bio\\_chem\\_fac\\_pubs/11](http://digitalcommons.liberty.edu/bio_chem_fac_pubs/11)

# Peri-nuclear clustering of mitochondria is triggered during aluminum maltolate induced apoptosis

David A. DeWitt<sup>a,b,\*</sup>, Jennifer A. Hurd<sup>a</sup>, Nena Fox<sup>b</sup>, Brigitte E. Townsend<sup>a</sup>, Kathleen J.S. Griffioen<sup>a,c</sup>, Othman Ghribi<sup>d</sup> and John Savory<sup>b</sup>

<sup>a</sup>*Department of Biology, Liberty University, Lynchburg, VA, USA*

<sup>b</sup>*Department of Pathology, University of Virginia, Charlottesville, VA, USA*

<sup>c</sup>*Department of Pharmacology and Physiology, George Washington University, Washington, DC, USA*

<sup>d</sup>*Department of Pharmacology, University of North Dakota, Grand Forks, ND, USA*

**Abstract.** Synapse loss and neuronal death are key features of Alzheimer's disease pathology. Disrupted axonal transport of mitochondria is a potential mechanism that could contribute to both. As the major producer of ATP in the cell, transport of mitochondria to the synapse is required for synapse maintenance. However, mitochondria also play an important role in the regulation of apoptosis. Investigation of aluminum (Al) maltolate induced apoptosis in human NT2 cells led us to explore the relationship between apoptosis related changes and the disruption of mitochondrial transport. Similar to that observed with tau over expression, NT2 cells exhibit peri-nuclear clustering of mitochondria following treatment with Al maltolate. Neuritic processes largely lacked mitochondria, except in axonal swellings. Similar, but more rapid results were observed following staurosporine administration, indicating that the clustering effect was not specific to Al maltolate. Organelle clustering and transport disruption preceded apoptosis. Incubation with the caspase inhibitor zVAD-FMK effectively blocked apoptosis, however failed to prevent organelle clustering. Thus, transport disruption is associated with the initiation, but not necessarily the completion of apoptosis. These results, together with observed transport defects and apoptosis related changes in Alzheimer disease brain suggest that mitochondrial transport disruption may play a significant role in synapse loss and thus the pathogenesis or Alzheimer's disease.

Keywords: Apoptosis, axonal transport, Alzheimer's disease, aluminum, staurosporine

## 1. Introduction

Disrupted axonal transport may account for some unique features of Alzheimer's disease including neuritic dystrophy, synapse loss, and the abnormal accumulation of phosphorylated tau in the neuronal soma [38, 39]. However, the regulation of axonal transport has received relatively little attention compared to other aspects of the disease despite several studies proposing

a role for disrupted transport. For example, axoplasmic flow disturbances together with accumulation of smooth ER have been observed in biopsy tissue from AD brain [31], and the Golgi apparatus is fragmented in non-tangle bearing neurons in AD [35]. In another study, neuritic striation was observed in AD brain where neuronal processes showed breaks with no cytoskeletal elements present instead of continuous filaments [44]. Further results comparing autopsy and biopsy AD tissue revealed cytoskeletal abnormalities indicating defective fast axonal transport [29]. Affected neurons in AD exhibit a reduced number of mitochondria, possibly due to the failure to transport them through the axons [16] and a reduced number of microtubules [4]. Moreover, Dai [7] demonstrated that neurons obtained

\*Corresponding author: David A. DeWitt, Ph.D., Dept. of Biology, Liberty University, 1971 University Blvd., Lynchburg, VA 24502, USA. Tel.: +1 434 582 2228; Fax: +1 434 582 2488; E-mail: dadewitt@liberty.edu.

from the temporal cortex of post mortem AD cases exhibit decreased axonal transport, and the degree of impaired transport was directly related to the degree of neuropathological changes.

Apoptosis has been suggested to play a role in AD [6, 36], however, the exact role it plays in neuropathology is unclear. For example, in affected neurons in AD, either the full apoptotic cascade is not activated, or apoptosis appears to have been aborted [25,26,30]. One possibility is that mitochondria are a key player linking the initiation of apoptosis and transport disruption. Indeed, peri-nuclear clustering of mitochondria is a distinct consequence of apoptosis related transport disruption. Concanavalin A induces apoptosis in a murine macrophage cell line and triggers peri-nuclear clustering of mitochondria [37]. TNF- $\alpha$  [22] and TNF-Related Apoptosis Inducing Ligand (TRAIL) [41] both induce clustering of mitochondria as an initial step in triggering apoptosis. Indeed, TNF induces the hyperphosphorylation of kinesin light chains which effectively inhibits transport [9]. Interestingly, one consequence of tau over-expression is peri-nuclear clustering of mitochondria and the failure of normal kinesin dependent transport [10,33,43].

Previous work has established that intracisternal injection of Al maltolate can trigger neurofibrillary pathology, apoptosis and oxidative damage in aged rabbits [32]. In this model Al maltolate initiates apoptosis involving both the endoplasmic reticulum (ER) and the mitochondria [12], consistent with increasing evidence that suggests signaling between the ER and mitochondria may be involved in the regulation of programmed cell death [13,14]. Further, the release of cytochrome c triggered by Al maltolate administration is blocked by Cyclosporine A, a specific inhibitor of the mitochondrial permeability transition pore [11]. Co-administration of glial derived neurotrophic factor (GDNF) with Al maltolate resulted in the upregulation of Bcl-2 and the inhibition of mitochondrial translocation of Bax effectively preventing apoptosis [12]. In addition there was no increase in caspase-3 activity or TUNEL positive nuclei following GDNF administration. Interestingly, despite reduced neurological symptoms and apoptosis related changes following GDNF administration, cytochrome c release still occurs, indicating apoptosis is blocked downstream of cytochrome c release. Therefore, apoptosis related changes are clearly implicated in the neuropathological changes in this model and specifically mitochondria are especially vulnerable to these effects.

To validate the applicability to AD, we have extended the rabbit model and developed an *in vitro* model us-

ing human NT-2 cells [15]. Previously we have confirmed that Al maltolate triggers substantial cell death. Further, cell death occurs by apoptosis, as evidenced by TUNEL positive nuclei, nuclear fragmentation and cytochrome c release. The aim of the present study was to determine whether apoptosis is linked to transport disruption; specifically we asked whether Al maltolate induces peri-nuclear clustering of mitochondria, whether this effect is specific to Al maltolate, and examined whether organelle clustering precedes or follows apoptosis.

## 2. Materials and methods

### 2.1. Cell culture

DMEM/F-12 with 10% (v/v) FBS, 2 mM L-glutamine and 1% (v/v) penicillin-streptomycin was used as growth media for human teratocarcinoma (NT2) precursor cells. Cells were grown on glass coverslips in 6 well plates and maintained in 5% CO<sub>2</sub> at 37°C. Cells were plated and allowed to adhere and grow for 24 hours before use in experiments. These cells were differentiated following the procedure of Zigova [47]. Briefly, NT2 precursor cells were grown for 6 weeks with 10  $\mu$ M retinoic acid (Sigma) and cryopreserved with DMSO in liquid nitrogen prior to use.

### 2.2. Cell treatments

**Aluminum** – Al maltolate was prepared as described previously [3]. A stock solution of 25 mM Al maltolate was freshly prepared in sterile water and sterilized by passing it through a 0.2  $\mu$ m filter. Al maltolate was then added to growth medium for a final concentration of 500  $\mu$ M. Cells were incubated in Al maltolate or control media for 6 or 24 hours. In order to determine the effects of pulse exposure, a pulse of 500  $\mu$ M was administered for 2 hours and then replaced with fresh growth media. For lower Al concentrations, 500  $\mu$ M Al maltolate was serially diluted with growth media to 100  $\mu$ M, 25  $\mu$ M and 5  $\mu$ M. For an additional control, 1.5 mM maltolate was also used.

**Peroxide** – Hydrogen peroxide was used as a control to determine the specificity of Al induced organelle clustering. A stock solution of 30% H<sub>2</sub>O<sub>2</sub> (Sigma) was filter sterilized and diluted to 0.03% with growth media. Following an incubation of 30 minutes, peroxide containing media was replaced with fresh growth media.

**Staurosporine** – Staurosporine was used to determine whether organelle clustering was a characteristic of apoptosis in NT2 cells. A stock solution of 1 mM in DMSO (Sigma) was diluted to 450 nM with growth media. Cells were incubated in staurosporine containing media or vehicle alone for 2 or 24 hours.

**Nocodazole** – In order to determine whether an intact microtubule array was required for mitochondrial clustering, the anti-mitotic drug, nocodazole (Sigma) was used. Following 6 or 24 hours, control and Al maltolate treated cells were incubated with 5  $\mu$ M nocodazole for 30 minutes prior to cell labeling.

**z-VAD-FMK** – In order to determine whether active caspases were required for the clustering of mitochondria, NT2 cells were incubated with 20  $\mu$ M z-VAD-FMK (Promega) along with Al maltolate or staurosporine.

### 2.3. Mitochondrial labeling

To visualize mitochondria, cells were incubated for 20 minutes in 200 nM CMXRos and/or 200 nM Mito-Tracker Green (Molecular Probes) following treatment with Al maltolate. After incubation in mitochondrial dyes at 37°C, cells were then quickly washed with sterile PBS, and fixed in 4% formaldehyde for 20 minutes. Cells were rinsed and mounted with Vectasheild mounting media (Vector Laboratories) or processed for immunocytochemistry.

### 2.4. Immunocytochemistry

Fixed cells were rinsed with PBS and then permeabilized with ethanol:acetic acid 19:1 or 0.2% Triton X 100. An antibody to  $\beta$ -tubulin (Sigma) was used to determine the cell size and distribution of this cytoskeletal protein. Biotinylated secondary and FITC conjugated avidin (Vector Laboratories) was used. Cells were mounted with Vectasheild with DAPI (Vector Laboratories) to visualize the nucleus. Images were obtained using a Zeiss Axioskop 2 plus fluorescent microscope with a SPOT camera.

### 2.5. Quantitation

The percentage of cells with clustered mitochondria was determined by obtaining an average from four random fields per coverslip with 2–4 coverslips per treatment group, performed in triplicate. Total cells were obtained as well as the number where mitochondria appeared to be accumulated in the vicinity of the nu-

cleus rather than spread throughout the cell. For a cell to count as having clustered mitochondria, a very high density of the organelle juxtaposed to the nucleus was required with large areas of the cell essentially devoid of mitochondria. In most cases, two independent observers were used to quantify the clustered phenotype with similar results. Cells which had clearly shrunk with an apoptotic morphology were included in the cell number, but were not counted as clustered. To assist in the determination of clustering, composite images showing mitochondria (CMXRos)  $\beta$ -tubulin and/or DAPI were used for comparison. Statistical significance was determined using a one way ANOVA on Microsoft Excel.

### 2.6. Neuritic density of mitochondria

NT2 cells were differentiated with retinoic acid and then treated with 500  $\mu$ M Al maltolate, 450 nM staurosporine or control media for up to 24 hr. Cells were incubated with CMXRos for mitochondria and immunostained for  $\beta$ -tubulin for the total neurite area. Neuritic density of mitochondria was determined in 100x images using the NIH Image J program. Pixel area for mitochondria was compared to the total neurite area ( $\beta$ -tubulin). Swollen neurites were excluded from analysis. Statistical significance was determined using a one way ANOVA on Microsoft Excel.

## 3. Results

### 3.1. Aluminum maltolate triggers mitochondrial clustering

Treatment with 500  $\mu$ M Al maltolate induced cell death in NT2 cells. Nuclei typically exhibited a fragmented morphology consistent with apoptosis. CMXRos positive mitochondria were observed in both control and Al maltolate treated cultures. In controls, mitochondria tended to be thin, elongated and distributed relatively evenly throughout the cell (Fig. 1A). Mitochondria in cells treated with maltol alone were indistinguishable from that of control cells (Fig. 1B). However, following incubation for 24 hours in 500  $\mu$ M Al maltolate, mitochondrial morphology and distribution dramatically changed; mitochondria tended to be fragmented, swollen and round. Importantly, mitochondria also clustered in the peri-nuclear region near the vicinity of the presumed microtubule organizing center (Fig. 1C, and 1D). Mitochondrial clustering of-

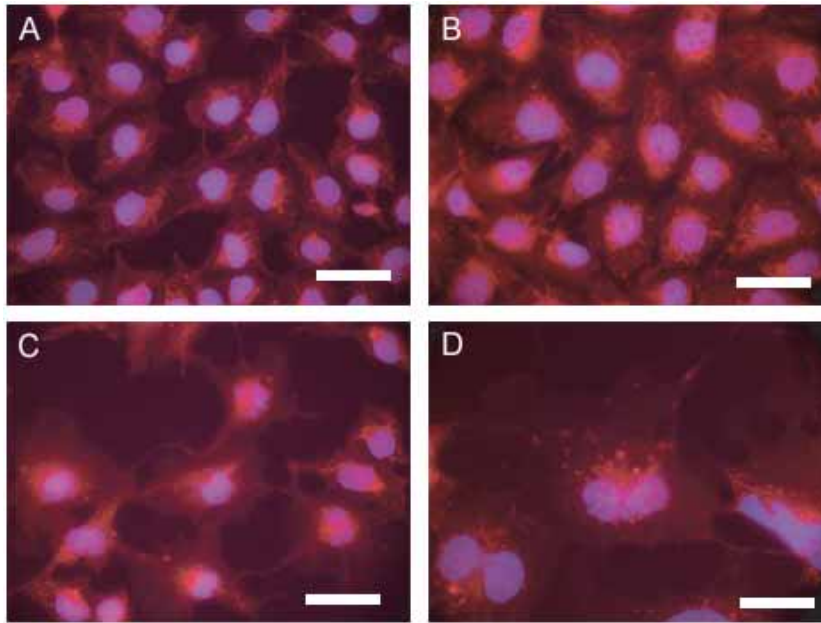


Fig. 1. Al maltolate induces peri-nuclear clustering of mitochondria. CMXRos (red) reveals the cellular distribution of mitochondria. In control NT-2 cells (A) or maltolate alone (B), mitochondria have a long, thin morphology and are distributed throughout the cell. Following incubation in 500  $\mu\text{M}$  Al maltolate for 24 hr, (C, D) mitochondria tend to be clustered near the nucleus. This is especially apparent at higher magnification (D) where mitochondria appear fragmented (arrow) compared to controls. Immunocytochemistry for cytochrome c revealed the same pattern. Scale bar (A, B, C) = 50  $\mu\text{m}$ , (D) = 20  $\mu\text{m}$ .

ten coincided with nuclear fragmentation suggesting a relationship to apoptosis. However, mitochondrial clustering appears to be an early event since cells with mitochondrial aggregates were observed with an intact nucleus. Thus, mitochondrial clustering precedes nuclear fragmentation. At six hours of incubation, there was no significant difference in the percentage of mitochondrial clustered cells between control and aluminum treated cells. Although there was some variation, at 24 hours in Al maltolate consistently > 50% of the remaining cells had clustered mitochondria. Cells in advanced stages of apoptosis were shrunken and therefore were not counted as clustered, thus reducing the percentage of clustered cells.

Exposure to Al maltolate for 2 hours did not lead to significant death or mitochondrial clustering. However, pulse exposure of two hours followed by incubation for a total of 24 hours did in fact lead to death and mitochondrial clustering (Fig. 2). Both cell death and mitochondrial clustering was slightly reduced compared to continuous exposure to Al maltolate. Lower doses of Al maltolate (5 to 100  $\mu\text{M}$ ) did not result in significant cell death or mitochondrial clustering after 24 hours consistent with effective concentrations in other studies [20]. These results are consistent with a threshold dose of Al required to trigger apoptosis.

### 3.2. A subpopulation of mitochondria lose membrane potential with Al maltolate

Loss of mitochondrial membrane polarity often precedes the release of cytochrome c and further activation of the apoptosis cascade. Therefore, we investigated whether Al maltolate triggered mitochondrial depolarization. CMXRos is a mitochondrial dye that is taken up only by mitochondria with intact membrane polarity. In contrast, MitoTracker green is taken up by all mitochondria. Therefore, polarized mitochondria will accumulate both dyes whereas depolarized mitochondria will only take up MitoTracker green.

In control cultures, MitoTracker Green and CMXRos overlapped indicating that essentially all of the mitochondria are polarized (Fig. 3A). However, mitochondria from Al maltolate treated cells exhibited a subset of mitochondria which were depolarized (Fig. 3B). Depolarized mitochondria were typically found in the vicinity of the nucleus.

### 3.3. Mitochondrial clustering requires an intact microtubule array

Peri-nuclear clustering of mitochondria may be a result of decreased kinesin transport relative to dynein

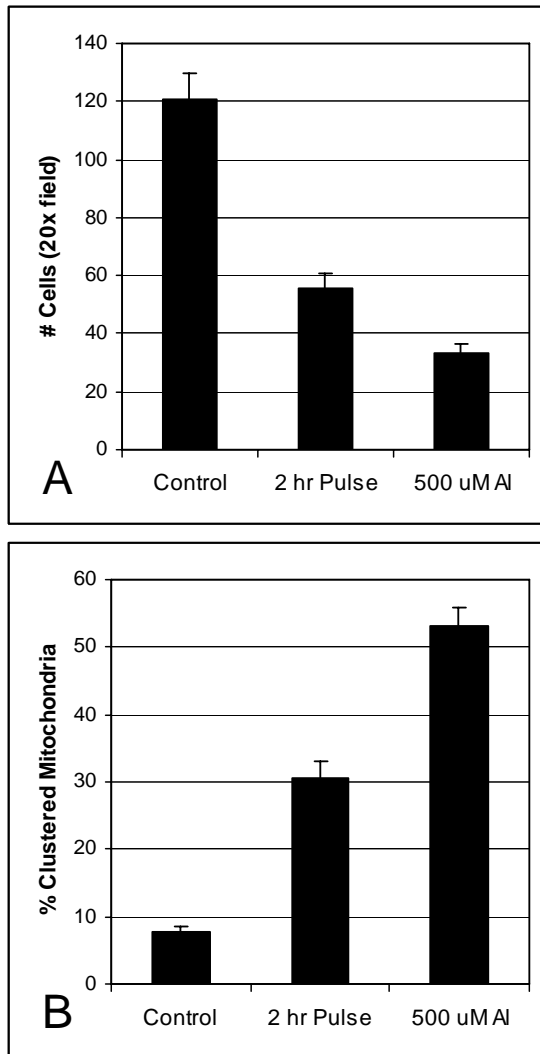


Fig. 2. Pulse exposure of Al maltolate triggers apoptosis and transport abnormalities. NT-2 cells exposed to a pulse of 500  $\mu$ M Al maltolate for 2 hr, and then allowed to grow in control media show significant cell death (A) and mitochondrial clustering (B) although not to the extent of continuous Al maltolate exposure (B). Cells which appeared shrunken were not counted as clustered.  $\pm$  SD  $p < 0.005$ .

transport along microtubules. Therefore, if the transport of mitochondria to the peri-nuclear region is an active process, it would require at least a partially intact microtubule array to carry them. After incubation for 24 hours in 500  $\mu$ M Al maltolate, cells were exposed to 5  $\mu$ M nocodazole for 30 minutes. Nocodazole initiated a rapid breakdown of the microtubule cytoskeleton and resulted in a redistribution of mitochondria within the cell and peri-nuclear clustering was virtually abolished (Fig. 4).

### 3.4. Z-VAD-FMK, a caspase inhibitor does not prevent mitochondrial clustering

Since organelle clustering during apoptosis induction could result from downstream activity of caspases, we incubated NT2 cells with z-VAD-FMK (20  $\mu$ M) along with Al maltolate or staurosporine. Although cell death was reduced, nuclear fragmentation and mitochondrial clustering persisted (Fig. 5). In particular, the nucleus appeared hyperlobated. This suggests that although mitochondrial clustering occurs during the induction of apoptosis, it is a caspase independent process.

### 3.5. Staurosporine but not hydrogen peroxide induces rapid mitochondrial clustering

In order to determine the specificity of Al induced organelle clustering, we investigated whether other agents that induce apoptosis also triggered mitochondrial clustering. Treatment with 450 nm staurosporine also led to cell death through apoptosis. CMXRos positive mitochondria indicated that the membrane polarity of mitochondria remained intact following staurosporine treatment. Mitochondrial clustering was observed in virtually every cell as early as 2 hours, much more rapidly than with Al treatment (Fig. 6). Although relatively few cells were left after 24 hours, many of those remaining did not exhibit mitochondrial clustering.

Hydrogen peroxide treatment at 0.03% for 30 minutes induced substantial cell death. Unlike Al treatment which results in nuclei with a fragmented morphology, nuclei in peroxide treated cells were condensed and significantly smaller. Indeed, overall cell size was dramatically reduced preventing the determination of mitochondrial clustering in peroxide treated cells (Data not shown).

### 3.6. Neuritic processes of treated cells are depleted of mitochondria

A functional consequence of decreased kinesin dependent transport in differentiated neurons would be the failure to transport mitochondria to the synapse. Such failure would be expected to produce catastrophic results including loss of the synapse and possibly cell death. Therefore, we examined the mitochondrial density in the neuritic processes of differentiated NT-2 cells following Al maltolate administration.

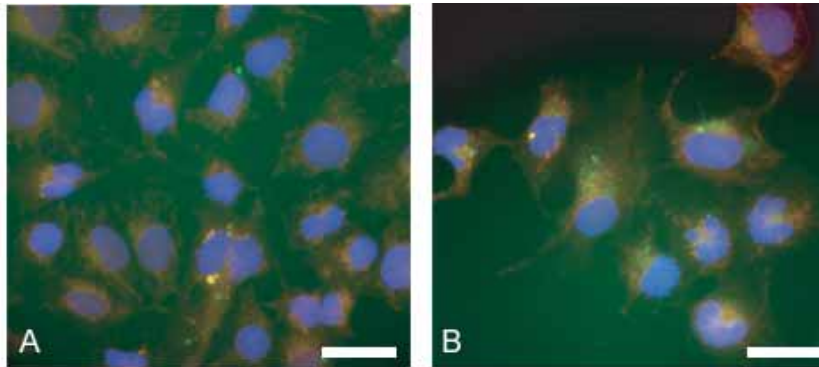


Fig. 3. Al maltolate induces mitochondrial membrane polarity loss in a subset of the mitochondria. NT-2 cells were incubated with both CMXRos (red) and MitoTracker Green. In control cells, mitochondria take up both dyes (A) shown by orange overlap. Following a 24-hr incubation in Al maltolate, a subset of mitochondria are depolarized, revealed by the presence of MitoTracker green, and lack of CMXRos. The depolarized mitochondria tended to be in greatest abundance near the nucleus (DAPI, blue). Scale bar = 50  $\mu$ m.

Differentiated cells (dNT2) will elaborate neuronal processes that contain neurofilament protein, tubulin and mitochondria. Following treatment with 500  $\mu$ M Al maltolate for 24 hr, a substantial number of the cells were lost, presumably through apoptosis. Surviving cells with long neuritic processes typically had large axonal swellings, some of which had a large amount of mitochondria. Apart from these axonal swellings, processes of surviving cells had a substantially reduced density of mitochondria (Fig. 7).

After a two hour treatment with 450 nM staurosporine, dNT2 cells had an altered morphology which included numerous branched neuritic processes. As with Al maltolate, these processes were depleted of mitochondria or exhibited neuritic swellings with accumulated mitochondria. In nearly all cells that survived treatment with staurosporine for 24 hours, mitochondria were accumulated and condensed into a large dense mass on one side of the nucleus.

#### 4. Discussion

In this study we have demonstrated that the apoptosis inducing agents Al maltolate and staurosporine both trigger peri-nuclear clustering of mitochondria in human NT2 cells. Further, these agents induce an overall lack of mitochondria in neuronal processes of differentiated cells. The clustering of mitochondria often precedes nuclear fragmentation and thus is considered an early event during apoptosis. In addition, the caspase inhibitor z-VAD-FMK prevented cell death but not organelle clustering, an effect most pronounced in staurosporine treated cells.

Numerous studies have demonstrated that aluminum is a prominent apoptotic agent. Molecular mechanisms of aluminum-induced apoptosis vary according to the aluminum salt, the dose, exposure time, and the cell type used. In human peripheral-blood lymphocytes, Al Cl<sub>3</sub> induces DNA damage by modifying the structure of chromatin through the induction of reactive oxygen species or by damaging lysosomal membranes and liberating DNase [2]. Exposure of rat PC12 cells to aluminum maltolate resulted in depletion of glutathione, resulting in release of lactate dehydrogenase (LDH) from the cell and generation of reactive oxygen species. These effects were reversed by pretreatment with N-acetylcysteine [33]. Treatment of Neuro-2a cells with Al maltolate for 24 h dose-dependently increased cell death by a combination of apoptosis and necrosis. Apoptosis was evident by caspase 3 activation, the externalization of phosphatidyl serine, inhibition of Bcl2 expression and an increase in BAX as well as p53 expression [18]. Oral [17] or intracisternal injection [46] of aluminum to rat has also been shown to cause apoptosis. Interestingly, the aluminum-induced DNA fragmentation and caspase-3 and caspase-12 activation was prevented by co-administration of glial cell line-derived neurotrophic factor (GDNF) and exacerbated by brain-derived neurotrophic factor (BDNF), suggesting that neurotrophic factors may modulate the neurotoxic effects of aluminum [46]. Additionally, chronic aluminum exposure in rabbits enhances lipid peroxidation production and inhibits the superoxide dismutase (SOD) enzyme, effects that can be reversed by melatonin [1].

The role of mitochondrial clustering during the cell death cascade is unclear. Mitochondrial clustering alone is not required for cell death, as not all apoptotic

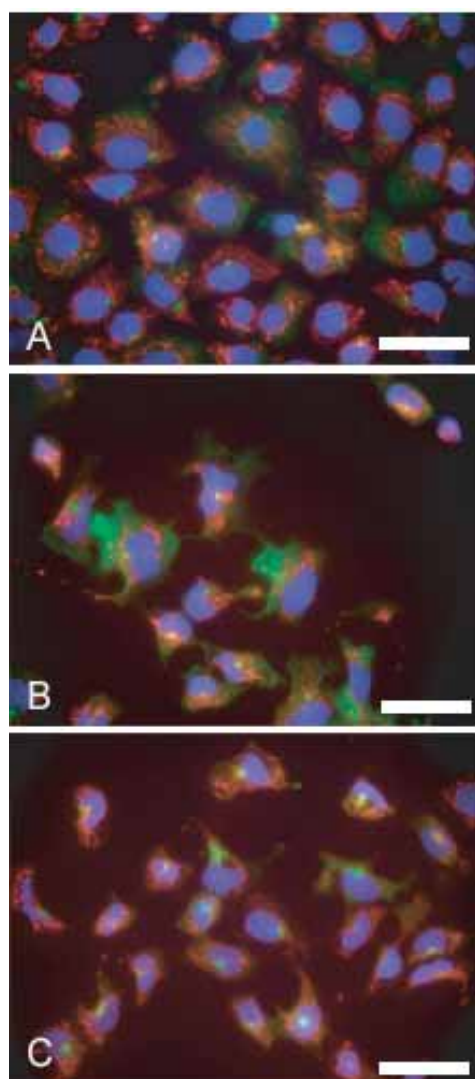


Fig. 4. Mitochondrial clustering requires intact microtubule based transport. Control NT-2 cells typically have mitochondria (CMXros, red) distributed throughout the cell (A). Mitochondria cluster near the nucleus (DAPI, blue) following incubation with 500  $\mu\text{M}$  Al maltolate for 24 hr (B). Al maltolate treatment followed by nocodazole resulted in a redistribution of mitochondria (C). Cell morphology is revealed by an antibody to  $\beta$ -Tubulin (green). Scale Bar = 50  $\mu\text{m}$ .

pathways involve peri-nuclear accumulation of the organelle (like  $\text{H}_2\text{O}_2$ ). However peri-nuclear mitochondrial aggregation likely hastens cell death as observed with  $\text{TNF}\alpha$  induced apoptosis [22]. Notably, consistent with our results,  $\text{TNF}\alpha$  clustering occurs in a caspase independent apoptotic process. Further, similar to Al maltolate and staurosporine, the  $\text{TNF}\alpha$  induced apoptotic pathway includes hyperlobated rather than condensed nuclei.

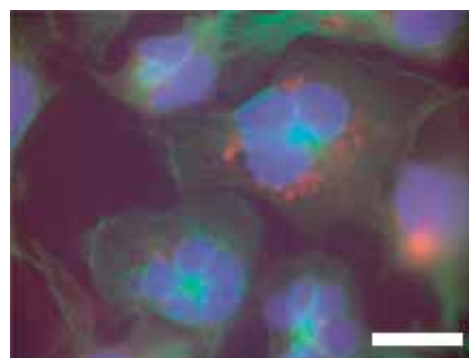


Fig. 5. Caspase inhibitor z-VAD-FMK does not prevent mitochondrial clustering. NT2 cells were treated with 500  $\mu\text{M}$  Al maltolate for 24 hrs in the presence of the caspase inhibitor Z-VAD-FMK (20  $\mu\text{M}$ ). Although cell death was reduced, nuclear fragmentation (DAPI, blue) and mitochondrial clustering (CMXros, red) persisted. There is also significant staining for  $\beta$ -Tubulin (green) in the center of the cells. Scale Bar = 20  $\mu\text{m}$ .

Recent studies on transgenic mice with fluorescently tagged neuronal mitochondria have been used to study axonal transport of mitochondria *in vivo* [23]. In these mice, large accumulations of mitochondria in synaptic terminals are observed as well as a high speed ( $> 1 \mu\text{m/s}$ ) of mitochondrial transport. Because of the significant requirement of mitochondria at the synapse, the failure to transport sufficient mitochondria into the axons and dendrites not only starve the synapse, but also slow or eliminate transport within the axon altogether. The absence of mitochondria in neuronal processes may lead to a localized depletion of ATP and slow or block transport, exacerbating the transport dysfunction. This loss of ATP in the axon, may contribute to overall transport failure including that of autophagic vesicles and thus facilitate the production of  $\text{A}\beta$  [45].

A surprising result from the present study was the observation that a pulse exposure of Al maltolate at 500  $\mu\text{M}$  effectively induced mitochondrial clustering, whereas prolonged exposure to Al maltolate at lower concentrations failed to induce identical effects. This result suggests that there exists a threshold signal, which when activated, initiates the apoptotic cascade and mitochondrial clustering. In contrast, staurosporine induced cell death and mitochondrial aggregation at much lower concentrations ( $\sim 1000\times$  lower). Although both Al maltolate and staurosporine result in cell death and mitochondrial clustering, there is an important distinction in cell morphology following administration of the two agents. In particular, both differentiated and undifferentiated cells treated with staurosporine showed significant elaboration of neuritic processes. Due to the length of the neurites, they are un-

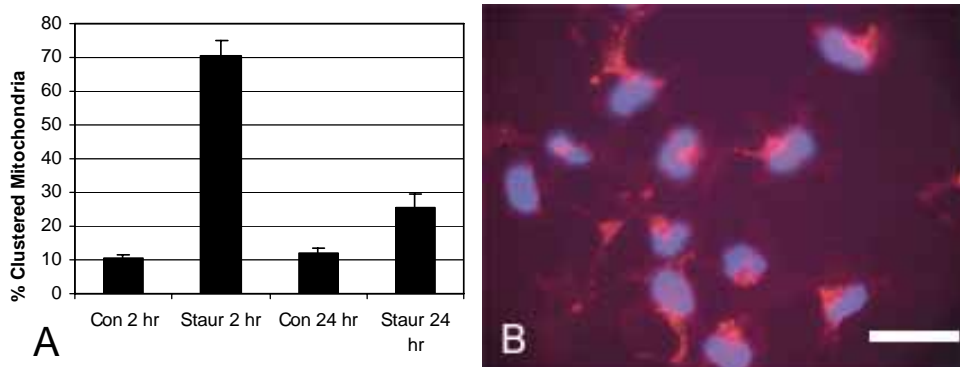


Fig. 6. Staurosporine induces mitochondrial clustering and apoptosis in NT2 cells. Incubation with 450 nM staurosporine triggers rapid clustering of mitochondria as early as 2 hr (A). A smaller percentage of cells showed mitochondrial clustering after 24 hr, however the total number of remaining cells was significantly reduced. CMXRos (red) reveals the mitochondria are clustered near the nucleus after 2 hr (DAPI, blue) in B. The morphology of the staurosporine treated cells was different from Al maltolate in that neuritic processes were prominent although mostly devoid of mitochondria. Values are  $\pm$  SD,  $p < 0.001$ .

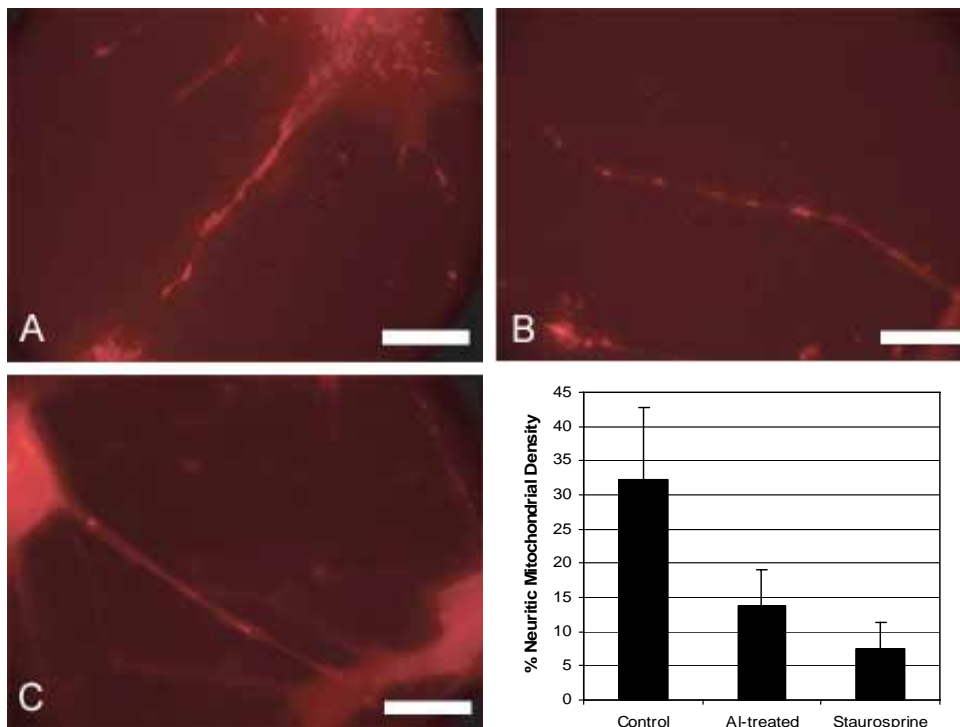


Fig. 7. Neuritic processes of differentiated cells have reduced mitochondria after Al maltolate or staurosporine treatment. NT-2 cells extend neuritic processes after differentiation with retinoic acid. In control cells, (A) these processes tend to have large numbers of mitochondria (CMXRos, red) throughout. However, with Al maltolate treatment (B, 500  $\mu$ M for 24 hr) the density is reduced except in swollen regions. With 450 nM staurosporine treatment, very few mitochondria are present in neuritic processes (C). Quantitation of mitochondrial density shows a significant decrease of mitochondria (D). Control  $n = 56$ , Al-treated  $n = 52$ , Staurosporine treated  $n = 20$ .  $\pm$  SD  $p < 0.001$ , Scale bar = 20  $\mu$ M.

likely to result simply from incomplete cell shrinkage. Indeed, staurosporine triggers the elaboration of neurites in PC-12 cells [24]. Staurosporine is a broad spectrum kinase inhibitor and may prevent the phospho-

rylation of tau. Unphosphorylated tau strongly binds and stabilizes microtubules, which can result in both the elongation of neuritic processes *and* the prevention of kinesin transport. In the absence of sufficient

mitochondrial transport, the neuron will be unable to sustain the axon and synapse. Therefore, it is possible that the over-phosphorylation of tau may be an attempt to restore appropriate levels of mitochondrial transport through axons.

Recently, it has been shown that  $A\beta$  induced neurotoxicity is dependent on the increased expression of both tau and cdk5 [26]. Importantly,  $A\beta$  results in decreased AKT activity, which in turn leads to increased GSK3 $\beta$  activity and a possible increase in tau phosphorylation [5]. AKT is a survival-promoting kinase that inhibits GSK3 $\beta$  by phosphorylating it on Ser(9). Guanosine protects cells from staurosporine and  $A\beta$  induced apoptosis presumably by increasing the phosphorylation/activation of AKT [27]. While apoptosis-related changes are clearly implicated in AD, the exact role that it plays in neuropathology and in the disruption of mitochondrial transport remains to be elucidated.

In addition to evidence from AD brains, several disease models have also suggested the involvement of transport abnormalities in neuropathological changes. Transgenic mice expressing human *ApoE4* in neurons exhibit axonal dilations with accumulated organelles [40]. Failure of axonal transport is further implicated in AD since the  $A\beta$ PP protein binds directly to kinesin, a microtubule motor protein responsible for positive directed transport [19]. Indeed,  $A\beta$ PP may be a cargo receptor for kinesin. Coexpression of tau and APPL, the *Drosophila* homologue of  $A\beta$ PP, in neurons resulted in disrupted transport of axonal cargo [42]. Indeed, the overexpression of APPL shares many similarities with mutations in the kinesin heavy chain gene. Further, in presenilin 1 mutant transgenic mice [28] and 3XTG-AD transgenic mice [8], there are early disruptions in axonal transport and reduced synaptic density.

We propose that disruption to mitochondrial transport and the subsequent loss of ATP is a significant precipitating factor for the pathogenesis of AD. Failure to transport sufficient mitochondria through axons may have a major contribution to synapse loss and neuronal death.

## Acknowledgements

This work was supported by the National Institutes of Health grant AG-020996 and the Jeffress Memorial Trust.

## References

- [1] S.Kh. Abd-Elghaffar, G.H. El-Sokkary and A.A. Sharkawy, Aluminum-induced neurotoxicity and oxidative damage in rabbits: protective effect of melatonin, *Neuro Endocrinol Lett* **26** (2005), 609–616.
- [2] A. Banasik, A. Lankoff, A. Piskulak, K. Adamowska, H. Lisowska and A. Wojcik, Aluminum-induced micronuclei and apoptosis in human peripheral-blood lymphocytes treated during different phases of the cell cycle, *Environ Toxicol* **20** (2005), 402–406.
- [3] R.L. Berthol, M.M. Herman, J. Savory, R.M. Carpenter, B.C. Sturgill, C.D. Katsetos, S.R. Vandenberg and M.R. Wills, A long-term intravenous model of aluminum maltol toxicity in rabbits: tissue distribution, hepatic, renal, and neuronal cytoskeletal changes associated with systemic exposure, *Toxicol Appl Pharmacol* **98** (1989), 58–74.
- [4] A.D. Cash, G. Aliev, S.L. Siedlak, A. Nunomura, H. Fujioka, X. Zhu, A.K. Raina, H.V. Vinters, M. Tabaton, A.B. Johnson, M. Paula-Barbosa, J. Avila, P.K. Jones, R.J. Castellani, M.A. Smith and G. Perry, Microtubule reduction in Alzheimer's disease and aging is independent of tau filament formation, *Am J Pathol* **162** (2003), 1623–1627.
- [5] A. Cedazo-Minguez, B.O. Popescu, J.M. Blanco-Millan, S. Akterin, J.J. Pei, B. Winblad and R.F. Cowburn, Apolipoprotein E and beta-amyloid (1-42) regulation of glycogen synthase kinase-3beta, *J Neurochem* **87**(5) (2003), 1152–1164.
- [6] C.W. Cotman and A.J. Anderson, A potential role for apoptosis in neurodegeneration and Alzheimer's disease, *Mol Neurobiol* **10**(1) (1995), 19–45.
- [7] J. Dai, R.M. Buijs, W. Kamphorst and D.F. Swabb, Impaired axonal transport of cortical neurons in Alzheimer's disease is associated with neuropathological changes, *Brain Res* **948** (2002), 138–144.
- [8] A. Deshpande, R. Resende, P. Helguera, S. Oddo, I. Smith, F. LaFerla and J. Busciglio, Mitochondrial dysfunction and transport defects in 3XTG-AD mice. Program No. 83.15. 2005 Abstract Viewer/Itinerary Planner. Washington, DC: Society for Neuroscience, 2005, online.
- [9] K. De Vos, F. Severin, F. Van Herreweghe, K. Vancompernelle, V. Goossens, A. Hyman and J. Grooten, Tumor Necrosis Factor Induces Hyperphosphorylation of Kinesin Light Chain and Inhibits Kinesin-mediated Transport of Mitochondria, *J Cell Biol* **149** (2000), 1207–1214.
- [10] A. Ebner, R. Godemann, K. Stamer, B. Illenberger, B. Trinczek and E. Mandelkow, Overexpression of tau protein inhibits kinesin-dependent trafficking of vesicles, mitochondria and endoplasmic reticulum: implications for Alzheimer's disease, *J Cell Biol* **143**(3) (1998), 777–794.
- [11] O. Ghribi, D.A. DeWitt, M.S. Forbes A. Arad, M.M. Herman and J. Savory, Cyclosporin A inhibits Al-induced cytochrome c release from mitochondria in aged rabbits, *J Alzheim Dis* **3**(4) (2001), 387–391.
- [12] O. Ghribi, M.M. Herman, M.S. Forbes, D.A. DeWitt and J. Savory, GDNF protects against aluminum-induced apoptosis in rabbits by upregulating Bcl-2 and Bcl-XL and inhibiting mitochondrial Bax translocation, *Neurobiol Dis* **8**(5) (2001), 764–773.
- [13] O. Ghribi, D.A. DeWitt, M.S. Forbes, M.M. Herman and J. Savory, Co-involvement of mitochondria and endoplasmic reticulum in regulation of apoptosis: changes in cytochrome c, Bcl-2 and Bax in the hippocampus of aluminum-treated rabbits, *Brain Res* **903**(1–2) (2001), 66–73.

- [14] O. Ghribi, M.M. Herman, D.A. DeWitt, M.S. Forbes and J. Savory, Abeta(1-42) and aluminum induce stress in the endoplasmic reticulum in rabbit hippocampus, involving nuclear translocation of gadd 153 and NF-kappaB, *Brain Res Mol Brain Res* **96**(1-2) (2001), 30-38.
- [15] K.J.S. Griffioen, O. Ghribi, N. Fox, J. Savory and D.A. DeWitt, Aluminum induced toxicity occurs through apoptosis and includes cytochrome c release, *Neurotoxicol* **25** (2004), 859-867.
- [16] K. Harai, G. Aliev, A. Nunomura, H. Fujioka, R.L. Russell, C.S. Atwood, A.B. Johnson, Y. Kress, H.V. Vinters, M. Tabaton, S. Shimohama, A.D. Cash, S.L. Siedlak, P.L.R. Harris, P.K. Jones, R.B. Peterson, G. Perry and M.A. Smith, Mitochondrial abnormalities in Alzheimer's disease, *J Neurosci* **21**(9) (2001), 3017-3023.
- [17] J.W. Huh, M.M. Choi, J.H. Lee, S.J. Yang, J. Choi, K.H. Lee, J.E. Lee and S.W. Cho, Activation of monoamine oxidase isotypes by prolonged intake of aluminum in rat brain, *J Inorg Biochem* **99** (2005), 2088-2091.
- [18] V.J. Johnson, S.H. Kim and R.P. Sharma, Aluminum-maltolate induces apoptosis and necrosis in neuro-2a cells: potential role for p53 signaling, *Toxicol Sci* **83** (2005), 329-339.
- [19] A. Kamal, A. Almenar-Queralt, J.F. LeBlanc, E.A. Roberts and L.S. Goldstein, Kinesin-mediated axonal transport of a membrane compartment containing beta-secretase and presenilin-1 requires APP, *Nature* **414**(6864) (2001), 643-648.
- [20] Y. Kashiwagi, Y. Nakamura, Y. Miyamae, R. Hashimoto and M. Takeda, Pulse exposure of cultured rat neurons to aluminum maltol affected the axonal transport system, *Neurosci Lett* **252** (1998), 5-8.
- [21] T. Liu, G. Perry, H.W. Chan, G. Verdile, R.N. Martins, M.A. Smith and C.S. Atwood, Amyloid-beta-induced toxicity of primary neurons is dependent upon differentiation-associated increases in tau and cyclin-dependent kinase 5 expression, *J Neurochem* **88**(3) (2004), 554-563.
- [22] N.A. Maianski, D. Roos and T.W. Kuijpers, Tumor necrosis factor  $\alpha$  induces a caspase-independent death pathway in human neutrophils *Blood* **101**(5) (2003), 1987-1995.
- [23] T. Misgeld, M. Kerschensteiner, F. Bareyre and J.W. Lichtman, Transgenic mice with fluorescently tagged neuronal mitochondria as a new tool to study axonal transport *in vivo* Program No. 369.4. 2005 Abstract Viewer/Itinerary Planner, Washington, DC: Society for Neuroscience, 2005, online.
- [24] R. Nuydens, G. Dispertsyn, M. de Jong, G. van den Kieboom, M. Borgers and H. Geerts, Aberrant tau phosphorylation and neurite retraction during NGF deprivation in PC-12 cells, *Biochem Biophys Res Commun* **240**(3) (1997), 687-691.
- [25] G. Perry, A. Nunomura and M.A. Smith, A suicide note from Alzheimer disease neurons? *Nature Medicine* **4**(8) (1998), 897-898.
- [26] G. Perry, A. Nunomura, P. Lucassen, H. Lassmann and M.A. Smith, Apoptosis and Alzheimer's Disease, *Science* **282** (1998), 1268-1269.
- [27] K.M. Pettifer, S. Kleywegt, C.J. Bau, J.D. Ramsbottom, E. vertes, R. Ciccarelli, F. Caciagli, E.S. Wesluc and M.P. Rathbone, Guanosine protects SH-SY5y cells against beta-amyloid-induced apoptosis, *Neuroreport* **15**(5) (2004), 833-836.
- [28] G. Pigino, G. Morfini, A. Pelsman, M.P. Mattson, S.T. Brady and J. Busciglio, Alzheimer's Presenilin 1 Mutations Impair Kinesin-Based Axonal Transport, *J Neurosci* **23**(11) (2003), 4499-4508.
- [29] D. Praprotnik, M.A. Smith, P.L. Richey, H.R. Vinters and G. Perry, Filament heterogeneity within the dystrophic neurites of senile plaques suggests blockage of fast axonal transport in Alzheimer's disease, *Acta Neuropathol (Berl)* **91**(3) (1996), 226-235.
- [30] A. K. Raina, A. Hochman, X. Zhu, C.A. Rottkamp, A. Nunomura, S.L. Siedlak, H. Boux, R.J. Castellani, G. Perry and M.A. Smith, Abortive apoptosis in Alzheimer's disease, *Acta Neuropathol (Berl)* **101**(4) (2001), 305-310.
- [31] S. Richard, J.P. Brion, A.M. Couck and J. Flament-Durand, Accumulation of smooth endoplasmic reticulum in Alzheimer's disease: New morphological evidence of axoplasmic flow disturbances, *J Submicrosc Cytol Pathol* **21**(3) (1989), 461-467.
- [32] J. Savory, J.K.S. Rao, P. Letada and M.M. Herman, Age-related hippocampal changes in Bcl-2:Bax ratio, oxidative stress, redox-active iron and apoptosis associated with aluminum-induced neurodegeneration: increased susceptibility with aging, *NeuroToxicol* **20** (1999), 805-818.
- [33] E. Satoh, M. Okada, T. Takadera and T. Ohyashiki, Glutathione depletion promotes aluminum mediated cell death of PC12 cells, *Biol Pharm Bull* **28** (2005), 941-946.
- [34] K. Stamer, R. Vogel, E. Thies, E. Mandelkow and E.M. Mandelkow, Tau blocks traffic of organelles, neurofilaments, and APP vesicles in neurons and enhances oxidative stress, *J Cell Biol* **156**(6) (2002), 1051-1063.
- [35] A. Stieber, Z. Mourelatos and N.K. Gonatas, In Alzheimer's disease the Golgi apparatus of a population of neurons without neurofibrillary tangles is fragmented and atrophic, *Am J Pathol* **148**(2) (1996), 415-426.
- [36] J.H. Su, G. Deng and C.W. Cotman, Bax protein expression is increased in Alzheimer's brain: correlations with DNA damage, Bcl-2 expression, and brain pathology, *J Neuropathol Exp Neurol* **56**(1) (1997), 86-93.
- [37] Y.K. Suen, K.P. Fung, Y.M. Choy, C.Y. Lee, C.W. Chan and S.K. Kong, Concanavalin A induced apoptosis in murine macrophage PU5-1.8 cells through clustering of mitochondria and release of cytochrome c, *Apoptosis* **5** (2000), 369-377.
- [38] R.D. Terry, Cell death or synaptic loss in Alzheimer Disease, *J Neuropathol Exp Neurol* **59**(12) (2000), 1118-1119.
- [39] R.D. Terry, The pathogenesis of Alzheimer disease: an alternative to the amyloid hypothesis, *J Neuropathol Exp Neurol* **55**(10) (1996), 1023-1025.
- [40] I. Tesseur, J. Van Dorpe, K. Bruynseels, F. Bronfman, R. Sciot, A. Van Lommel and F. Van Leuven, Prominent axon and disruption of axonal transport in transgenic mice expressing human apolipoprotein E4 in neurons of brain and spinal cord, *Am J Pathol* **157**(5) (2000), 1495-1510.
- [41] W.D. Thomas, X.D. Zhang, A.V. Franco, T. Nguyen and P. Hersey, TNF-Related Apoptosis-Inducing Ligand-Induced Apoptosis of Melanoma is Associated with Changes in Mitochondrial Membrane Potential and Perinuclear Clustering of Mitochondria, *J Immunol* **165** (2000), 5612-5620.
- [42] L. Torroja, H. Chu, I. Kotovsky and K. White, Neuronal overexpression of APPL, the Drosophila homologue of the amyloid precursor protein (APP), disrupts axonal transport, *Curr Biol* **9**(9) (1999), 489-492.
- [43] B. Trinczek, A. Ebner, E.M. Mandelkow and E. Mandelkow, Tau regulates the attachment/detachment but not the speed of motors in microtubule-dependent transport of single vesicles and organelles, *J Cell Sci* **112** (1999), 2355-2367.
- [44] M.E. Velasco, M.A. Smith, S.L. Siedlak, A. Nunomura and G. Perry, Striation is the characteristic neuritic abnormality in Alzheimer disease, *Brain Res* **813**(2) (1998), 329-333.
- [45] W.H. Yu, A.M. Cuervo, A. Kumar, C.M. Peterhoff, S.D. Schmidt, J.H. Lee, P.S. Mohan, M. Mercken, M.R. Farnery,

- L.O. Tjernberg, Y. Jiang, K. Duff, Y. Uchiyama, J. Naslund, P.M. Matthews, A.M. Cataldo and R.A. Nixon, Macroautophagy – a novel  $\beta$ -amyloid peptide-generating pathway activated in Alzheimer's disease, *J Cell Biol* **171** (2005), 87–98.
- [46] S.J. Yang, J.E. Lee, K.H. Lee, J.W. Huh, S.Y. Choi and S.W. Cho, Opposed regulation of aluminum-induced apoptosis by glial cell line-derived neurotrophic factor and brain-derived neurotrophic factor in rat brains, *Brain Res Mol Brain Res* **127** (2004), 146–149.
- [47] T. Zigova, L.F. Barroso, A.E. Willing, S. Saporta, M.P. McGrogan, T.B. Freeman and P.R. Sanberg, Dopaminergic phenotype of hNT cells *in vitro*, *Brain Res Dev Brain Res* **122** (2000), 87–90.

Copyright of Journal of Alzheimer's Disease is the property of IOS Press and its content may not be copied or emailed to multiple sites or posted to a listserv without the copyright holder's express written permission. However, users may print, download, or email articles for individual use.